ACCOUNTS
of chemical research

# π-Conjugated Cyanostilbene Derivatives: A Unique Self-Assembly Motif for Molecular Nanostructures with Enhanced Emission and Transport

BYEONG-KWAN AN,[†] JOHANNES GIERSCHNER,[‡] AND SOO YOUNG PARK*,[§]

[†]*Department of Chemistry, The Catholic University of Korea, Bucheon-si, Geyonggi-do 420-753, Korea,* [‡]*Madrid Institute for Advanced Studies, IMDEA Nanoscience, UAM, Modulo C-IX, AV. Tomásy Valiente 7, Campus de Cantoblanco, 28049 Madrid, Spain, and* [§]*Center for Supramolecular Optoelectronic Materials and WCU Hybrid Materials Program, Department of Materials Science and Engineering, Seoul National University, Seoul 151-742, Korea*

RECEIVED ON AUGUST 8, 2011

## CONSPECTUS

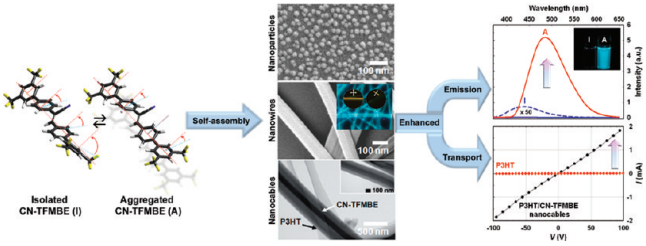


π-Conjugated organic molecules represent an attractive platform for the design and fabrication of a wide range of nano- and microstructures for use in organic optoelectronics. The desirable optical and electrical properties of π-conjugated molecules for these applications depend on their primary molecular structure and their intermolecular interactions such as molecular packing or ordering in the condensed states. Because of the difficulty in satisfying these rigorous structural requirements for photoluminescence and charge transport, the development of novel high-performance π-conjugated systems for nano-optoelectronics has remained a challenge.

This Account describes our recent discovery of a novel class of self-assembling π-conjugated organic molecules with a built-in molecular elastic twist. These molecules consist of a cyano-substituted stilbenic π-conjugated backbone and various terminal functional groups, and they offer excellent optical, electrical, and self-assembly properties for use in various nano-optoelectronic devices. The characteristic "twist elasticity" behavior of these molecules occurs in response to molecular interactions. These large torsional or conformational changes in the cyanostilbene backbone play an important role in achieving favorable intermolecular interactions that lead to both high photoluminescence and good charge carrier mobility in self-assembled nanostructures.

Conventional π-conjugated molecules in the solid state typically show concentration (aggregation) fluorescence quenching. Initially, we describe the unique photoluminescence properties, aggregation-induced enhanced emission (AIEE), of these new cyanostilbene derivatives that elegantly circumvent these problems. These elastic twist π-conjugated backbones serve as versatile scaffolds for the preparation of well-defined patterned nanosized architectures through facile self-assembly processes. We discuss in particular detail the preparation of 1D nanowire structures through programmed self-assembly.

This Account describes the importance of utilizing AIEE effects to explore optical device applications, such as organic semiconducting lasers (OSLs), optical memory, and sensors. We demonstrate the rich electronic properties, including the electrical conductivity, field-effect carrier mobility, and electroluminescence of highly crystalline 1D nanowire and coaxial donor–acceptor nanocable structures composed of elastic twist π-conjugated molecules. The electronic properties were measured using various techniques, including current–voltage (*I*–*V*), conducting-probe atomic force microscopy (CP-AFM), and space-charge-limited-current (SCLC) measurements. We prepared and characterized several electronic device structures, including organic field-effect transistors (OFETs) and organic light-emitting field-effect transistors (OLETs).



Published on the Web 11/15/2011 www.pubs.acs.org/accounts
10.1021/ar2001952 

## 1. Introduction

In recent years, π-conjugated organic molecules have been intensively developed as an attractive platform for the design and fabrication of a wide range of nano- and microstructures for use in organic optoelectronics. In particular, the controlled self-assembly of π-conjugated organic molecules and their use as functional building blocks by subtly balancing noncovalent intermolecular forces has gained increasing interest.[1] The desirable optical and electrical properties of π-conjugated molecules for optoelectronics are significantly controlled by intermolecular interaction parameters associated with molecular packing or ordering in the condensed states, no less than their primary molecular properties.[2]

Difficulties associated with predicting and controlling the effects of intermolecular interactions on the electrical and optical properties, however, have presented a challenge to the use of π-conjugated molecules as molecular building motifs in optical and electrical devices. Whereas charge transport is favored by dense ordered molecular stacking derived from strong π−π interactions,[2] such intermolecular interactions often lead to photoluminescence (PL) quenching due to concentration quenching phenomenon.[2] In addition to these issues, good solubility of π-conjugated molecules must also be compromised (without destroying the desired electrical and optical properties) for the fabrication of solution-processable optoelectronic devices via self-assembly.

Recently, our group developed a series of new π-conjugated molecules comprising a cyanostilbene backbone with terminal functional groups (Figure 1). The structural characteristics of these molecules have proven to be extremely beneficial in bestowing desirable electrical and photophysical properties on self-assembled materials in the context of organic optoelectronics. In particular, these molecules exhibit a unique "elastic twist" feature; that is, large torsional or conformational changes occur readily in response to intermolecular interactions. Isolated molecules in dilute solution are significantly twisted by internal steric repulsions; however, the low rotational energy penalty permits assumption of a more coplanar and conjugated conformation during the self-assembly process mediated by specific intermolecular interactions. The planar structure maximizes the π−π intermolecular interactions and thus greatly contributes to tight molecular packing, which in turn promotes charge transport. Importantly, the combined effects of aggregation-induced planarization and the specific head-to-tail molecular arrangement yield unprecedented optical properties, including aggregation-induced enhanced emission (AIEE), which ameliorates "aggregation (or concentration) quenching" in solid-state conjugated materials.[2] Despite the absence of bulky solubilizing alkyl groups, cyanostilbene molecules show good solubility in various common organic solvents due to the unique twist conformation and polar substituents. Another fascinating property of these molecules is their capacity for self-assembly to form a variety of nanoscale architectures as a result of the delicate balance among noncovalent forces between cyanostilbene-based backbones and terminal units.

In the following, we first describe the unique AIEE properties of cyanostilbene molecules and the structural relationships in the solid state. We next discuss the versatile uses of these molecules as molecular building blocks for the self-assembly of nanostructures in various dimensions, with emphasis on their patterned architectures. Finally, we highlight their characteristic optical and electrical properties as they relate to a variety of nano-optoelectronic device applications.

## 2. Aggregation-Induced Enhanced Emission (AIEE)

The absorption and emission properties of π-conjugated oligomers are defined by the inherent conjugated backbone, but these properties can change dramatically upon aggregation.[2,3] The factors responsible for such changes may include the solid environment, which generally inhibits large-amplitude intramolecular motions, and specific intermolecular interactions, which are preformed by the electronic and steric requirements of the molecules. For the majority of π-conjugated molecules, including stilbene-based systems, the main absorption band is formed by the $S_0 \rightarrow S_1$ transition, in which the molecular transition dipole moment $\mu$ is mainly oriented along the long molecular axis (Figure 2).[2,3] Hence, H-aggregation refers to side-by-side oriented molecules with small displacement along the long molecular axis. H-aggregate absorption spectra are hypsochromically (blue) shifted against the solution and exhibit low radiative rate constants $k_r$ due to the dipole-forbidden nature of the emitting state.[2,3] H-Aggregates commonly result in concentration quenching, which is observed for the majority of π-conjugated compounds in the solid state, although such compounds may be highly emissive in the

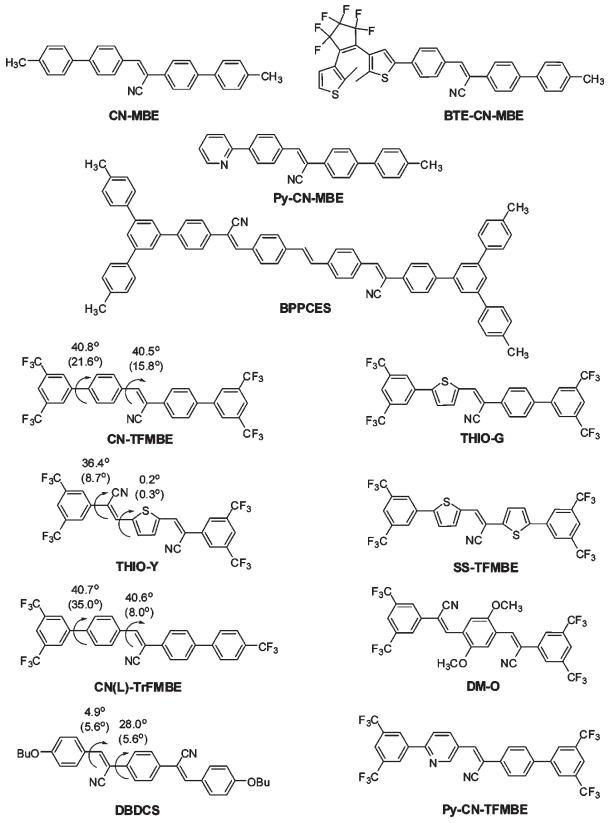


**FIGURE 1.** Molecular structures of cyanostilbene molecules and dihedral torsional angles in the isolated and single crystal states (in brackets).

isolated solution state. An increase of molecular displacement along the long molecular axis transforms a system from H- to J-aggregates. The latter displays bathochromic (red) shifted absorption and high $k_r$,[2,3] giving rise to a high solid-state PLQY.

**AIEE.** Contrary to the common concentration quenching described above, cyanostilbene molecules, for example, CN-MBE, show entirely opposite PL properties due to their unique twist elasticity. In solution, biphenyl and cyanostilbene units of CN-MBE are significantly twisted beyond 40° as a result of intramolecular repulsion among the ortho hydrogen atoms and bulky cyano moieties.[4] This twisted structure activates torsion-induced nonradiative deactivation by avoiding the planar quinoidal mesomeric conformation in the $S_1$ state,[5] thereby rendering the solution nonfluorescent, as shown in the inset of Figure 3b. In the condensed state, however, as observed for the colloidal nanoparticles of CN-MBE, strong intermolecular $\pi-\pi$ interactions contributed by the cyano groups cause conformational planarization of the twisted biphenyl and cyanostilbene units, and the planarization is strong enough to overcome the small rotational energy barrier at the central C−C bond of the biphenyl rings (<3.9 kcal/mol)[6] or the C−C bond between the phenyl ring

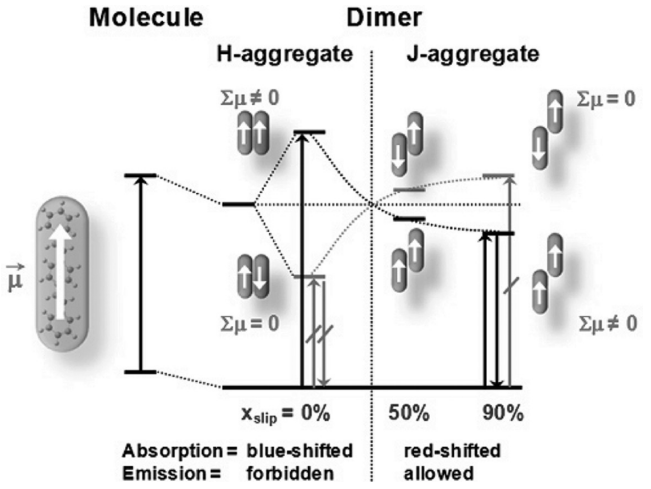


**FIGURE 2.** H- and J-aggregates and their impact on the absorption and emission processes in the framework of exciton models.

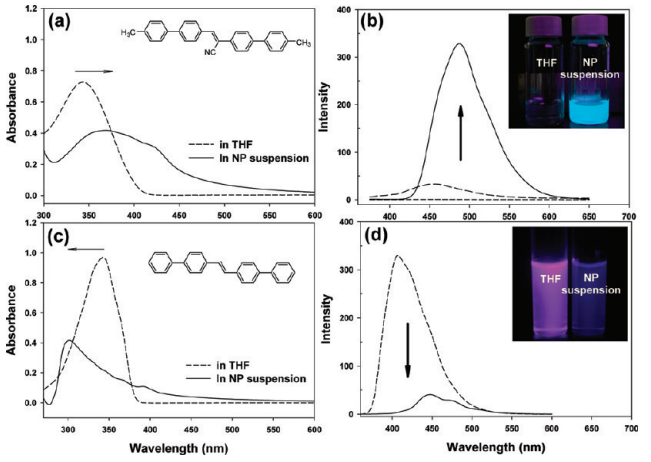


**FIGURE 3.** UV absorption and PL spectra of CN-MBE (a and b) and DPST (c and d) ($2 \times 10^{-5}$ M) in THF and NP suspensions (80 vol % water in THF), respectively.

and the central double bond of the stilbene units (<3.3 kcal/mol).[7] Single crystal X-ray diffraction (XRD) analysis of several other cyanostilbene molecules actually confirmed planarization during aggregation (Figure 1).

The aggregation-induced planarization extends the effective conjugation length (thus increasing the radiative rate $k_r$), but significantly suppresses nonradiative deactivation pathways at the same time. Consequently, aggregation-induced planarization significantly enhances the PLQY of CN-MBE from solution ($\Phi_{PL,sol}$ = 0.001) to nanoparticle suspension ($\Phi_{PL,\ NP}$ = 0.690) with concurrent bathochromic shift in the emission wavelength ($\lambda_{max,sol}$ = 455 nm → $\lambda_{max,NP}$ = 488 nm) (Figure 3b). A very high PLQY in the aggregated state suggests the presence of J-aggregates instead of H-aggregates. The latter are frequently found in

stilbene-based systems.[5] In fact, the absorption of an (optically thin) CN-MBE nanoparticle suspension ($\lambda_{max}$ = 368 nm) was bathochromically shifted relative to the solution state ($\lambda_{max}$ = 344 nm) (Figure 3a), indicative of J-aggregation. In contrast, H-type aggregation with a dramatic hypsochromic shift in the absorption and a reduced PLQY were observed for *trans*-4,4′-diphenylstilbene (DPST) (Figure 3c and d), which lacks only the cyano group from CN-MBE structure and thus shows a more planar π-conjugated backbone. It should be noted, however, that the cyanostilbene functionality does not always cause J-aggregation. For DBDCS, H-aggregation with hypsochromically shifted absorption and a low radiative rate is observed.[8] In contrast to DPST, however, the PLQY of DBDCS in the aggregated state is high ($\Phi_{PL,NP}$ = 0.62), ascribed to a low exciton trapping probability due to the uniform crystal structure induced by tight stacking among cyanostilbene motifs.

The synergistic combination of aggregation-induced planarization and specific intermolecular interactions results in dramatically enhanced emission upon aggregation, that is, the AIEE effect. AIEE opposes the notorious concentration PL quenching among π-conjugated molecules in the solid state and is a common feature of conjugated systems with cyanostilbene functionalities in the excited state.[9] The nature of AIEE is quite different from that of other enhanced emission phenomena observed, for example, in siloles (kinked aromatic molecules)[10] and arene-perfluoroarenes,[11] in which the solid-state PL enhancement derives only from restricted intramolecular rotational motion and exciplex formation, respectively. Finally, it is noteworthy that the AIEE of cyanostilbene molecules is not caused by special solvatochromic effects.[12,13]

## 3. Tailored Nanoengineered Structures and Morphologies

The combination of the cyanostilbene motif and a number of different substituents on the terminal rings subtly balances the noncovalent molecular forces, including π−π stacking, hydrogen bonding, and electrostatic interactions, which play essential roles in the formation of various types of nanostructures with controlled dimensions via spontaneous self-assembly. Introducing pyridine groups as self-assembly modulators can assist in the precise placement of well-defined ordered nanoscale architectures of cyanostilbene molecules on the selected substrate surface as a result of programmed self-assembly processes.

**Colloidal Fluorescent Organic Nanoparticles (NPs).** These were readily prepared by a simple reprecipitation method without surfactants.[5] The colloidal CN-MBE NP suspensions obtained from THF/water mixture (1:4 v/v) exhibited dramatically enhanced blue fluorescence emission ($\Phi_{f,\ NP}$ = 0.69) as a result of the AIEE mechanism.[4] In particular, these NPs formed fine spheres of diameter 30−40 nm (Figure 4a) and were very stable for long periods of time (at least 6 months) due to the presence of polar cyano groups, which conveyed a negative ζ potential. Other CN-MBE derivatives were used to obtain a variety of NP emission colors, including green (THIO-G),[14] yellow (THIO-Y),[14] orange (BPPCES),[12] and red (DM-R),[14] all of which displayed AIEE properties (Figure 4b).

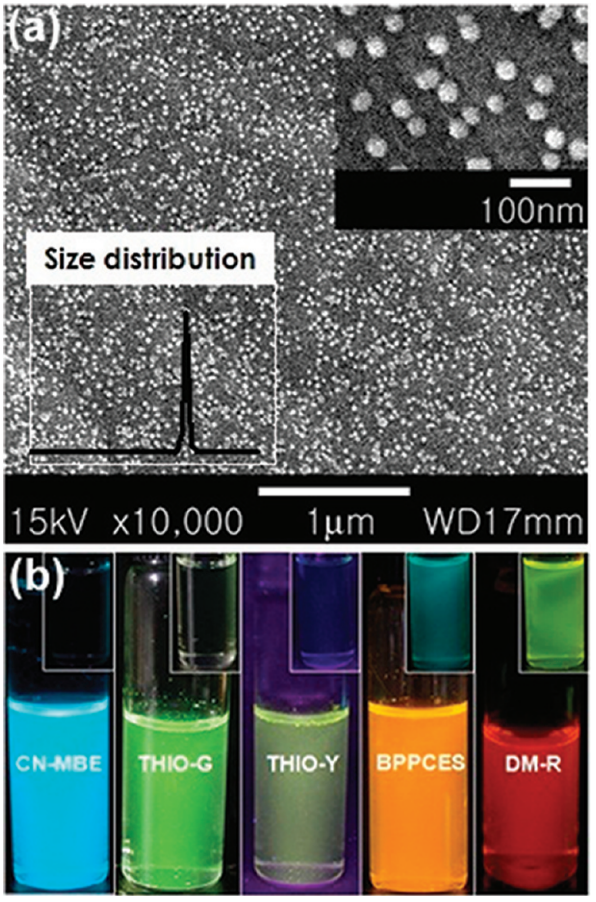


**FIGURE 4.** (a) SEM images and size distribution of CN-MBE NPs. (b) Fluorescence colors of the NP suspensions in THF/water (1:4 v/v): CN-MBE, THIO-G, THIO-Y, BPPCES, and DM-R, respectively (inset photos: the fluorescence colors in THF solutions).

**Highly Crystalline One-Dimensional (1D) Nanostructures.** These nanostructures were prepared from CN-TFMBE using various techniques, including drop-casting, vacuum evaporation, thermal annealing, and vapor-driven self-assembly (VDSA), all of which relied on the compounds' intrinsic capabilities with respect to 1D structural formation driven by the cyanostilbene backbone properties and the terminal $-CF_3$ units.[13,14] Ultralong self-assembled 1D

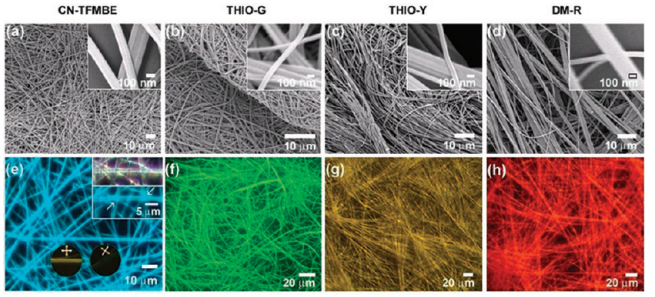


**FIGURE 5.** SEM and fluorescence microscopy images of CN-TFMBE (a and e), THIO-G (b and f), THIO-Y (c and g), and DM-R (d and h) NWs, respectively. The inset photos of (e) show the fluorescence of the underlying NWs projected through the higher NWs, and the circular inset photos show the birefringence of the NW bundles under crossed polarizers.

nanowires (NWs) with minimum diameters of 100 nm were bundled and arrayed over large areas of the substrate (Figure 5a). CN-TFMBE NWs showed bright blue PL ($\Phi_{f,\ NW} = 0.92$) (Figure 5e). They were transparent and exhibited strong birefringence under crossed polarizers, suggesting a high crystallinity that was further confirmed by XRD analysis. The combination of comprehensive XRD studies and multiscale computer simulations revealed the structural origins of highly crystalline 1D NWs,[14] which included (i) strengthening the electrostatic interactions among neighboring molecules via anisotropic electronic distributions induced by highly polar −CN groups, (ii) sliding the molecules along the molecular long axis by balancing steric repulsion and hydrogen bonding associated with the $-CF_3$ end groups, and (iii) constructing close and strong intermolecular $\pi-\pi$ stacking by aggregation-induced planarization. In the structural background of CN-TFMBE, we designed additional ultralong 1D NWs using THIO-G, THIO-Y, and DM-R (Figure 5b–d), which were used to tune the PL color in the NWs from green through yellow to red, respectively (Figure 5f–h).

**Flexible Two-Dimensional (2D) Unwoven Nanofabrics.** These nanofabrics were formed from NWs of CN-TFMBE and its derivative using a simple solution casting method. The resulting mechanically stable 2D nanofabrics were readily processed into various nano- or microarchitectures, such as 2D wrapped or multilayered 2D nanofabrics on curved substrates, by a modified soft deposition technique that took advantage of their excellent flexibility and mechanical properties (Figure 6a and b).[14] The surfaces of 2D nanofabrics were highly hydrophobic with water contact angles of 110–137°. The hydrophobicity could be increased up to 157°, yielding superhydrophobicity, by growing the nanowires perpendicular to the substrate surface (Figure 6c).[15]

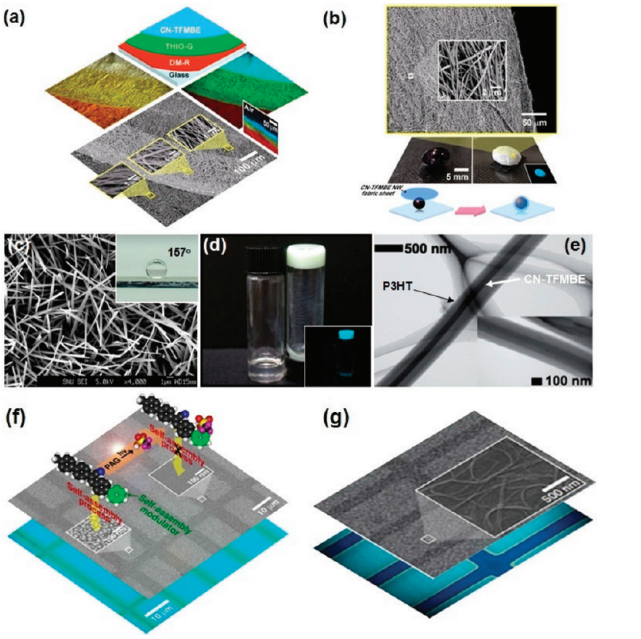


**FIGURE 6.** (a) Fluorescence microscopy and SEM images of multilayer structures of 2D-NFs deposited on glass substrates. (b) Photo and SEM images of the CN-TFMBE 2D-NFs deposited on a plastic ball substrate. (c) SEM image of vapor-deposited CN-TFMBE NWs on glass substrate (inset: a photo of water droplet onto the NW films). (d) Photo and fluorescence image (inset) of CN-TFMBE (0.8 wt/vol %) dissolved in 1,2-dichloroethane (left) and the corresponding organogel (right). (e) TEM image of coaxial nanocables of CN-TFMBE/P3HT. (f and g) Fluorescence emission and SEM images of photopatterned array of Py-CN-MBE NPs and Py-CN-TFMBE NWs in PMMA, respectively.

**3D Organogel Networks.** 3D organogel networks that did not flow under gravitational forces were created from CN-TFMBE and its derivatives, which formed bundles of 1D nanofibrous aggregates (Figure 6d).[13,14]

**Donor–Acceptor All-Organic Coaxial Nanocables.** These nanocables were fabricated from CN-TFMBE and regioregular polyhexylthiophene (P3HT) using a simple one-step solution process without the need for difficult synthetic approaches to covalently connect the donor (D) and acceptor (A) moieties.[16] Transmission electron microscopy (TEM) revealed that blending and annealing of P3HT and CN-TFMBE (50%–200% CN-TFMBE relative to P3HT; *o*-dichlorobenzene 0.1 wt % in solution) resulted in a structure in which P3HT spontaneously wrapped around the CN-TFMBE nanowires to form long uniform coaxial nanocables (Figure 6e). The polar cyanostilbene and $-CF_3$ units of CN-TFMBE play an important role in generating polar 1D NW cores, which effectively phase-demix from the nonpolar P3HT polymers, thereby inducing the concomitant formation of an outer polymer shell.

**Patterned Nanostructures via VDSA.** To realize the full potential of organic nanostructures in practical

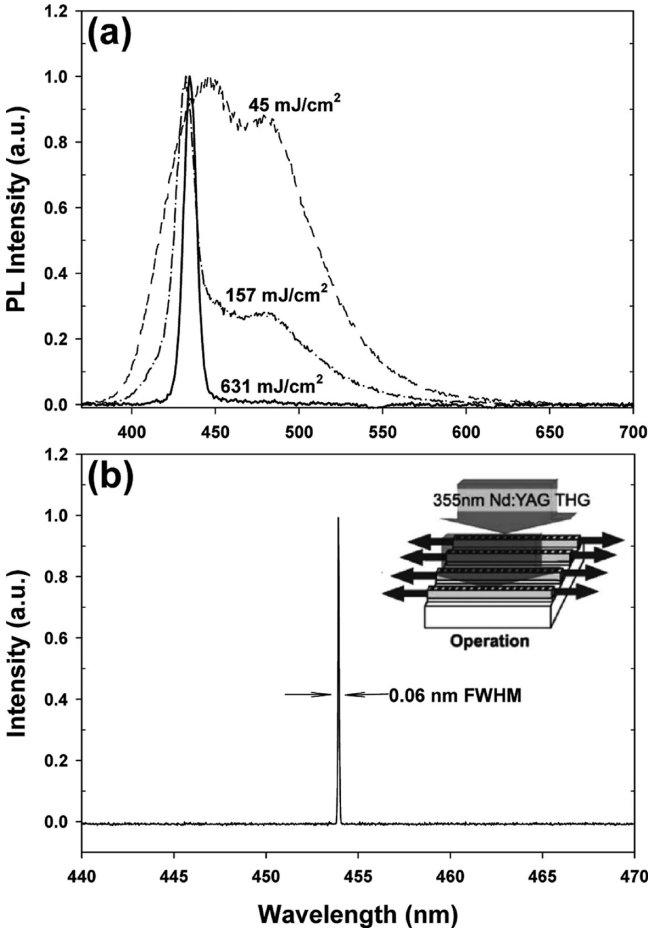


**FIGURE 7.** (a) ASE emission spectra of a CN-MBE:PMMA film pumped using a 355 nm UV pulse. (b) Spectral profile of the CN-MBE:PMMA DFB laser output.

nano-optoelectronic device applications, materials must be transferred to solid substrates and aligned within selected areas in a designed local configuration. Cyanostilbene molecules provide a solution to this challenge. CN-MBE NPs and CN-TFMBE NWs were readily fabricated directly in a poly(methyl methacrylate) (PMMA) polymer matrix using VDSA[17] (or solvent-vapor annealing (SVA))[18] methods, which relied on the selective phase-demixing and self-assembly of aggregates from a solid solution upon exposure to volatile organic solvent vapors. AIEE properties are useful for directly visualizing VDSA events because PL is instantly switched on during self-assembly. Importantly, randomly distributed CN-MBE NPs and CN-TFMBE NWs in a polymer matrix were patterned in selected areas upon chemical modification, for example, by replacing one phenyl unit in the cyanostilbene backbone with a pyridine ring unit as a self-assembly modulator during VDSA process.[17,18] The N atoms in the pyridine rings were readily protonated in the presence of photogenerated Brønsted acids, and Py-CN-MBE and Py-CN-TFMBE formed bulky quaternary salts with counterions ($X^- = CF_3SO_3^-$). The counterions eventually eliminated the capacity to self-assemble due to the bulkiness of the pyridine salt groups. Figure 6f and g shows that the formation of NPs and NWs was strictly localized in the neutral regions and was frustrated in the quaternized regions defined by the photolithography.

## 4. Optical Characteristics and Device Applications

The peculiar AIEE properties of cyanostilbene molecules are very useful and attractive for many optical device applications because they not only elegantly address the problem of concentration quenching in solid-state π-conjugated materials,[19] but they also provide large on/off PL ratios and dual emission color changes in response to external stimuli including solvent vapor, heat, and pressure,[20] which modulate intermolecular interactions.

**Robustly Distributed Feedback Dye Laser.** π-Conjugated fluorescent dyes are best known as active media for organic semiconducting lasers (OSLs). The direct use of these materials in the form of solid-state films is often not feasible due to significant PL quenching resulting from intermolecular interactions,[2] which leads to low optical gain cross sections. We investigated the amplified spontaneous emission (ASE) of these materials, which is a useful tool for exploring effective lasing conditions. The lasing action of CN-MBE-doped PMMA films prepared in a distributed feedback (DFB) structure was investigated.[21]

At low pump energies, the emissive spectra of the CN-MBE:PMMA films exhibited broad peaks corresponding to spontaneous emission, but a substantial reduction in the full-width at half-maximum (fwhm = 12 at 435 nm) was observed due to ASE at a pumping energy of 631 mJ/cm$^2$ (Figure 7a). The DFB waveguide structure showed excellent lasing properties with a maximum peak power of 5 W (threshold of 73 μJ/cm$^2$) and a fwhm of 0.06 at 454 nm (Figure 7b). More importantly, the robust cyanostilbene structure of CN-MBE yielded a lifetime of $1.7 \times 10^4$ shots. The outstanding durability of the CN-MBE DFB plastic blue laser was encouraging for practical applications because traditional blue organic laser dyes, such as coumarin 440, display rapid degradation (<100 shots) under UV irradiation.

**High-Contrast Nonvolatile Photochromic Optical Memory.** Bistable photoswitching of PL emission shows promise as a signaling mode for photon-mode molecular memory systems owing to the versatility of PL signals, including high-sensitivity and the absence of side effects that spoil the digitalized signals. However, concentration

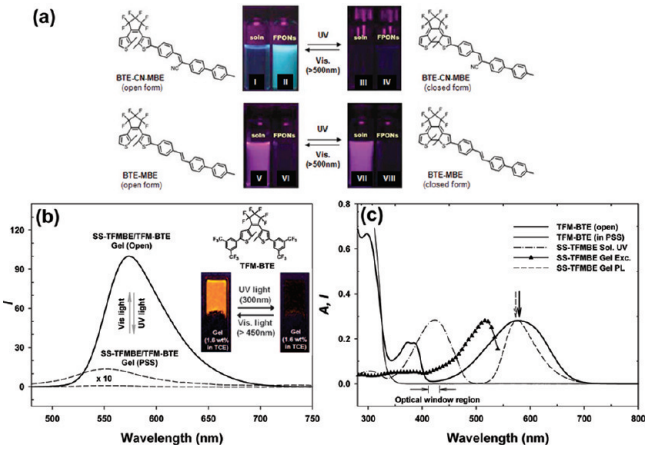


**FIGURE 8.** (a) Chemical structure and fluorescence changes of BTE-CN-MBE and BTE-MBE in a THF solution (soln) and in a colloidal suspension in THF/water (FPONs) upon ring-opening and closure of the BTE units. (b) PL spectral changes observed after the photochromic reaction of TFM-BTE with the SS-TFMBE organogel system. (c) Optical properties of TFM-BTE and SS-TFMBE.

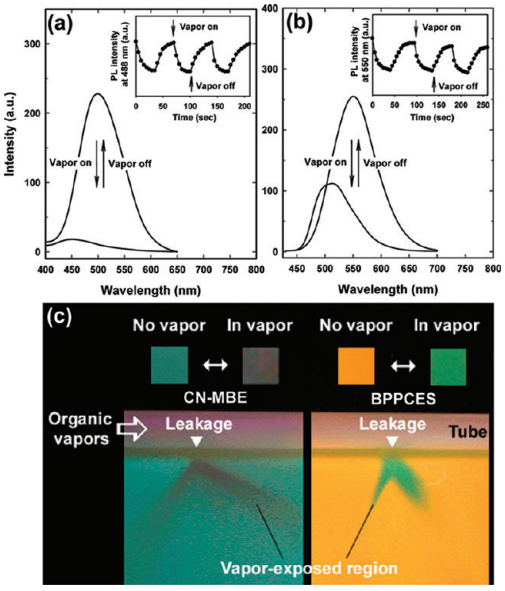


**FIGURE 9.** (a and b) PL spectral changes of CN-MBE and BPPCES adsorbed onto a TLC plate depending on the on/off flow of dichloromethane vapors, respectively. (c) Proof-of-concept vapor (dichloromethane) leak detection (0.5 mm hole) using CN-MBE and BPPCES adsorbed onto TLC plates.

quenching of PL signals remains a challenge and restricts the use of such materials in ultrahigh-density optical memory systems.

We demonstrated that the AIEE-active molecule BTE-CN-MBE can address this problem by incorporating a photochromic group, 1,2-bisthienylethene (BTE), into the CN-MBE backbone.[22] As in CN-MBE, BTE-CN-MBE NPs showed strongly enhanced PL, but were only weakly emissive in a THF solution due to AIEE (Figure 8a, I–II). This behavior was opposite to that of a non-AIEE analogue of BTE-MBE, which showed general concentration quenching in a NP suspension (Figure 8a, V–VI). Accompanied by the photochromic ring closure of BTE upon irradiation at 365 UV light, the PL intensity of BTE-CN-MBE NPs was greatly reduced as a result of intramolecular energy transfer (ET) to the closed-ring form of BTE (Figure 8a, III–IV). The maximum on/off PL intensity ratio of BTE-CN-MBE NPs exceeded 170 in the photostationary state, whereas that of the non-AIEE analogue of the BTE-MBE NPs showed only a 29% reduction in the PL intensity (Figure 8a, VII–VIII).

Although BTE-CN-MBE provided efficient reversible PL switching via intramolecular PL quenching, this system included several disadvantages: (i) difficulties associated with the design and synthesis and (ii) interference between the inherent photochromic properties of BTE and the fluorescent properties of the dyes, which caused destructive optical read-out processes. To address these problems, our efforts led us to develop a new cyanostilbene molecule, SS-TFMBE, which generates excellent organogels with an extremely bright yellow emission ($\lambda_{max}$ = 577 nm). The isolated SS-TFMBE in the sol state is almost nonfluorescent as a result of AIEE effects.[23] SS-TFMBE organogel was successfully utilized as a fluorescent reporter for optical memory systems upon direct doping with a new photochromic dye, TFM-BTE (ring closure and opening reactions under 300 nm UV light and >450 nm visible light illumination, respectively, Figure 8b inset), where the $-CF_3$ terminal units were introduced into the DTE backbone to achieve good compatibility with SS-TFMBE. The SS-TFMBE/TFM-BTE (2:1 wt %) mixed gel system was easily prepared, and the integrated PL intensity at 577 nm was significantly reduced (on/off PL switching ration >166) under 300 nm light illumination (Figure 8b) due to favorable spectral overlap between the PL spectrum of SS-TFMBE and the absorption spectrum of closed-form TFM-BTE (Figure 8c). This led to highly efficient intermolecular ET between SS-TFMBE and the closed-ring form of TFM-BTE (a "photon shutter" effect). Notably, the activated turn-on state was continuously preserved, regardless of the excitation number upon irradiation with 415 nm light for the PL read-out. Such "nonvolatile" memory characteristics were attributed to the characteristics of the optical window region in which the open- and closed-form TFM-BTE did not absorb, whereas PL excitation in SS-TFMBE aggregates was highly effective (over 410–432 nm).

**High-Performance Fluorescence Sensors for Volatile Organic Compounds (VOCs).** Conjugated materials may be especially beneficial in chemosensor and fluorescence

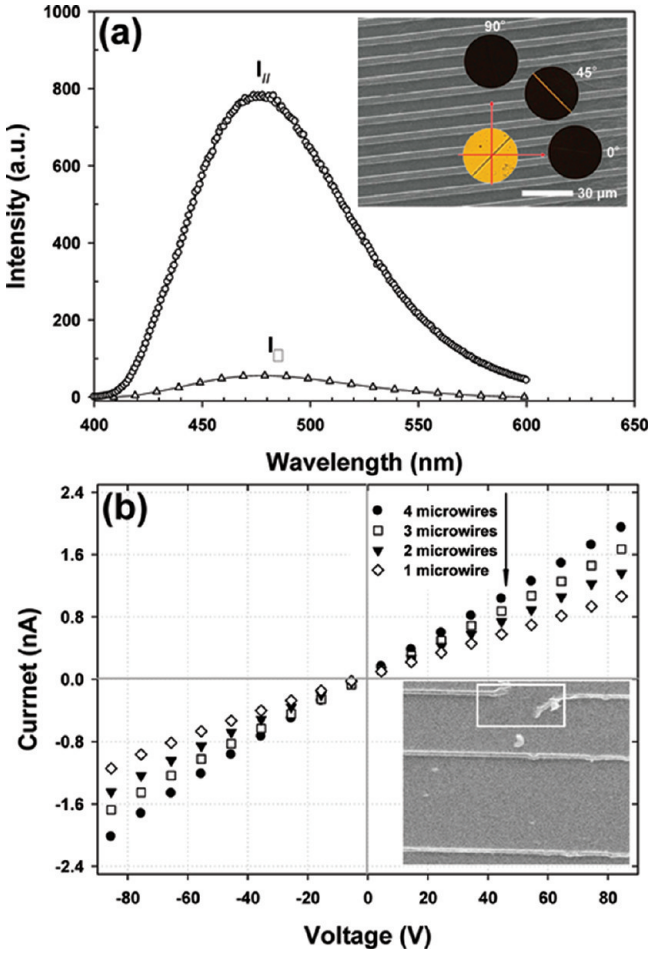


**FIGURE 10.** (a) Change in the PL intensity as a function of the angle between the direction of polarized film and that of patterned CN-TFMBE wires ($I_{//}$, parallel direction; $I_{\perp}$, perpendicular direction). Inset photos show SEM image of patterned CN-TFMBE NWs after MIMIC patterning and optical microscopy image of a single microwire under a cross-polarized film (circle image). (b) *I*–*V* curves measured for a smaller number of aligned wires (inset: SEM image of patterned and cutoff wires (inside rectangular circles)).

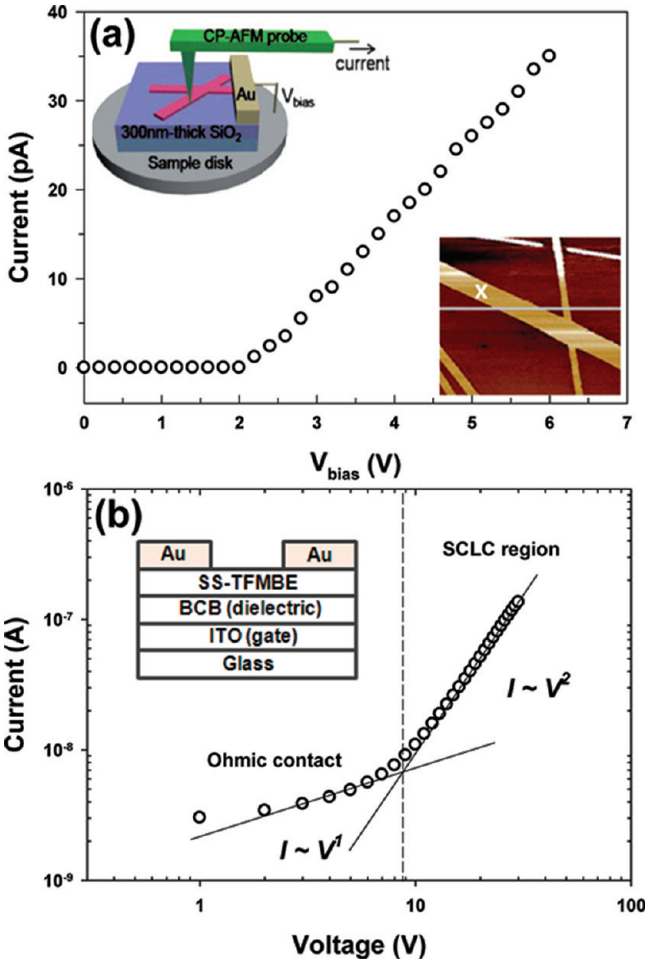


**FIGURE 11.** (a) Point current versus $V_{bias}$ at a fixed position on the SS-TFMBE NWs (indicated by an X in the inset) measured by CP-AFM experiments. (b) Log–log *I*–*V* plot of SS-TFMBE films measured at $V_G = 0$ V.

imaging[24] applications if their on/off or dual color PL switching properties can be controlled by external stimuli such as solvent vapors. CN-MBE and BPPCES molecules are well-suited for this purpose because of their salient PL modulation by AIEE; that is, isolated CN-MBE and BPPCES in solution provided virtually no fluorescence or green fluorescence, respectively, but showed high-intensity sky blue or orange emission in the aggregated states, respectively (Figure 4b).[12]

For practical uses in VOC sensor applications, CN-MBE and BPPCES molecules were adsorbed onto silica gel thin layer chromatography (TLC) plates, and they exhibited greenish blue and bright yellowish orange emission under 365 nm illumination. Exposure to dichloromethane vapors, however, resulted in a rapid quenching of the emission colors (a decrease by a factor of 24) or green emission (Figure 9), respectively, because the solvent vapor penetrated and weakened the intermolecular interactions, resulting in locally isolated molecules. The twist conformation of CN-MBE and BPPCES was, therefore, favored. The original bright and red-shifted emission spectra of CN-MBE and BPPCES in the aggregated state recovered completely upon removal of the vapor (Figure 9a and b insets).

## 5. Electrical Characteristics and Device Applications

The self-assembled highly crystalline 1D NWs of CN-TFMBE-type cyanostilbene molecules are fascinating objects for use in organic nanoelectronics as well as for fundamental electronic studies of organic semiconductors because highly ordered dense molecular stacking structures promoted effective charge transport by enhancing π-electronic communication among neighboring molecules. Moreover,

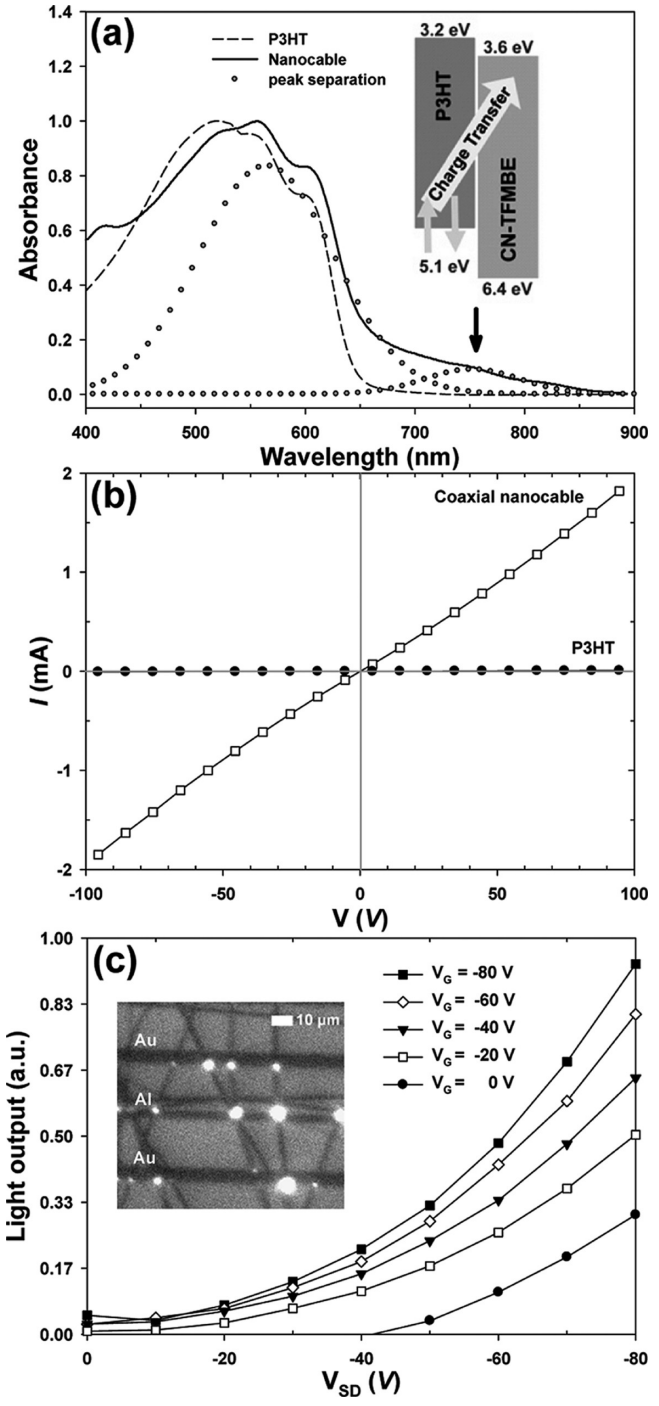


**FIGURE 12.** (a and b) UV/vis spectra and *I*−*V* characteristic of pristine P3HT and coaxial P3HT/CN-TFMBE nanocable films, respectively. (c) Light output versus $V_{SD}$ characteristics of the light-emitting transistor (inset: optical microscopy image of light emission from the coaxial nanocables during OFET operation).

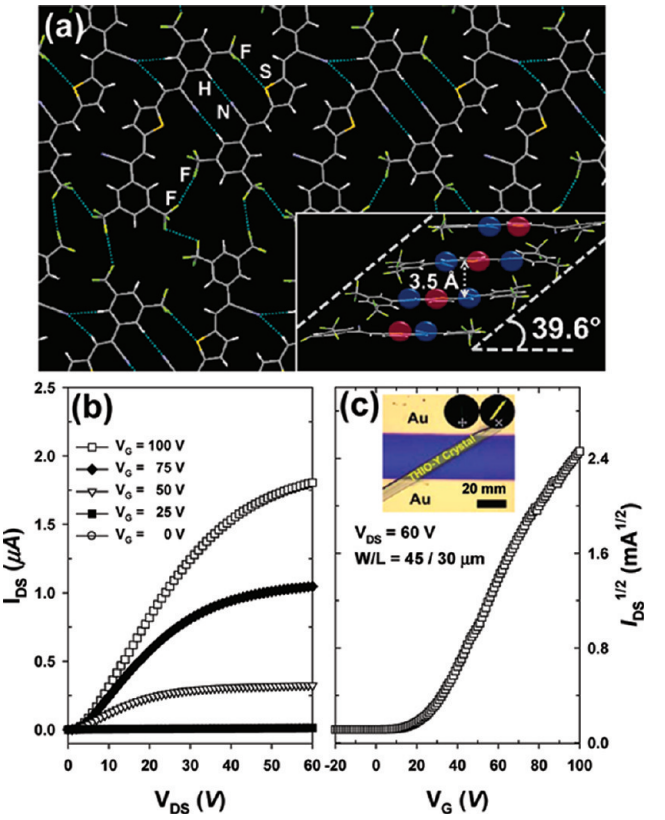


**FIGURE 13.** (a) Intermolecular interactions in the THIO-Y crystal (red circle, electron-rich thiophene ring; blue circle, electron-deficient CN unit). (b and c) Typical output and transfer characteristics of the THIO-Y single crystal OFETs, respectively (inset in (c): crystal device structure).

the compounds provide a promising platform for the construction of next-generation miniaturized electronic devices.

**Conductivity in Patterned Organic NW Electronic Devices.** The feasibility of using cyanostilbene NWs as key components in organic nanoelectronics was tested by examining the fundamental electrical properties of the CN-TFMBE NWs.[25] The patterned CN-TFMBE NWs by using a MIMIC (micromolding in capillaries) technique were aligned in a single direction toward the electrode channels (50 μm width), as confirmed by anisotropic optical studies (birefringence and polarized PL, Figure 10a). The current−voltage (*I*−*V*) characteristics of the micropatterned CN-TFMBE wires were recorded, giving a maximum calculated conductivity of $4.9 \times 10^{-6}$ S cm$^{-1}$ without doping processes, which was as high as the conductivity of $I_2$-doped poly(*p*-phenylene vinylene) (PPV) ($5.0 \times 10^{-6}$ S cm$^{-1}$).[26] The conductivity was directly proportional to the number of wires, as shown by consecutive cutting of individual wires (Figure 10b).

**Conductivity and Carrier Mobility in Single-Strand and Bulk Film Organic NWs.** Conducting-probe atomic force microscopy (CP-AFM) and space-charge-limited-current (SCLC) measurements are useful for locally characterizing the electrical properties of single strands and for measuring the intrinsic mobility (μ) of a bulk film, respectively. SS-TFMBE was characterized by using these techniques because of its capacity to self-assemble into rectangular-shaped highly

ordered crystalline 1D NWs that made good contact with AFM probe tips and Au electrodes (Figure 11a inset).[27]

A DC bias ($V_{bias}$) was applied to the fixed position of a single SS-TFMBE NW strand using an AFM probe tip and a top-contact Au electrode during CP-AFM measurements. The current flow along the physically contacted probe increased monotonically as the bias was increased above a critical value $V_{bias} = 2.0$ V, which strongly indicated that the NW was highly conductive (Figure 11a). The $I-V$ characteristics of a drop-cast NW film comprising SS-TFMBE in the quadratic regime (SCLC behavior region) ($|V| < 10$ V) provided an effective carrier mobility ($\mu_{eff}$) to give a maximum value of 3.1 $cm^2\ V^{-1}\ s^{-1}$ (Figure 11b).

**Enhanced Conductivity in an All-Organic Coaxial D−A Nanocable System.** Encouraged by the discovery of organic coaxial donor D−A nanocable architectures of CN-TFMBE/P3HT[16] as well as the favorable conducting properties of CN-TFMBE NWs mentioned above, we concentrated our interest in the conductive properties of CN-TFMBE/P3HT nanocables because this D−A nanocable system could provide an extended macroscopic coaxial D−A heterojunction over the whole length of the coaxial nanocables leading to improve the charge carrier mobility.

We found that a CT doping layer was formed at the heterojunction interface between CN-TFMBE (A) and P3HT (D), which facilitated electron transfer from the HOMO of P3HT (−5.1 eV) to the LUMO of CN-TFMBE (−3.6 eV). CT was experimentally characterized by the presence of an absorption band at 755 nm and an emission band at 824 nm (Figure 12a). The CT state formed an organic radical cation on the P3HT side ($D^{+\bullet}$) and a radical anion on the CN-TFMBE side ($A^{-\bullet}$) of the core−shell interface. Consequently, mobile charge carriers were produced by the CT process occurring at the interface between the core CN-TFMBE and the shell P3HT, and these carriers played a critical role in enhancing the electrical conductivity of the coaxial nanocables. To investigate the effects of mobile charge carriers on the electrical performance, the $I-V$ characteristics of coaxial nanocables and pristine P3HT film devices were measured and compared under a bias that ranged from −100 to 100 V. Measurements in 25 devices yielded highest and mean conductivities in the coaxial nanocable devices of 1.7 and 0.1 S $cm^{-1}$ (standard deviation: 0.078 S $cm^{-1}$), respectively, whereas those of the pristine P3HT devices were $2.8 \times 10^{-4}$ and $1.7 \times 10^{-4}$ S $cm^{-1}$ (standard deviation: $0.64 \times 10^{-4}$ S $cm^{-1}$), respectively (Figure 12b).

In addition, light emission was observed from the OFETs prepared using the coaxial nanocables as the active layer with interdigitated heteroelectrodes of gold and aluminum. Application of a gate voltage of −80 V yielded electroluminescence with an emission maximum peak at 700 nm only at the points on the nanocables at which the nanocables met the aluminum electrodes (hole−electron recombination zone) (Figure 12c). The intensity of the light output increased with the drain and gate voltage. These characteristics of coaxial OLETs were attributed to the efficient recombination of holes and electrons inside the nanocables.

**High-Performance *n*-Type Organic Transistors.** For high-performance *n*-type OFETs, electron-withdrawing groups incorporated into π-conjugated backbones result in efficient electron injection from electrodes due to lowered LUMO levels. However, the bulkiness and electrostatic forces introduced by these groups may destroy the highly crystalline structure or decrease the degree of molecular ordering. Therefore, the introduction of electron-withdrawing groups at appropriate positions in the π-conjugated building blocks is critical for securing both the desired high-crystallinity and the low LUMO level.

We found that THIO-Y met all prerequisites mentioned above due to its characteristic structural features, including high crystallinity and abundant electron-withdrawing units (two −CN and four $-CF_3$ groups).[28] XRD analysis revealed that the THIO-Y molecules were closely packed in a nearly coplanar fashion separated by an intermolecular distance of 3.5 Å. Notably, the −CN and $-CF_3$ groups not only effectively decreased the LUMO level of THIO-Y (−3.8 eV), which enhanced electron injection from the contact metals, but they also stabilized the laterally adjacent molecules by building up specific noncovalent intermolecular interactions, such as C−F···F−C, C−N···C−H (phenyl or vinyl), and C−F···S (thiophene ring) (Figure 13a). The dense molecular packing and appropriately low LUMO favored a good electron mobility in THIO-Y OFETs of as high as 0.16 $cm^2\ V^{-1}\ s^{-1}$ (Figure 13b and c).

## 6. Conclusions

The cyanostilbene system discussed in this Account offers a new approach to developing π-conjugated molecules that are useful as all-around building blocks for a variety of self-assembled organic nano-optoelectronics devices. This molecular system offers a solution to meet the rigorous demands of desired optical and electrical properties for nano-optoelectronics applications, as well as to control the nanoscale architecture. It should be noted that the characteristic

"twist elasticity" properties of these molecules play a significant role in governing the intermolecular interactions that achieve favorable electrical and optical properties, including high carrier mobilities and high PLQYs, as well as good solubilities.

*We thank all of the co-workers who have contributed to this research, especially as cited J. W. Chung, J. H. Kim, S.-J. Lim, S. J. Yoon, and Y. Oki. This research was supported by Basic Science Research Program (CRI; RIAMI-AM0209(0417-20090011)) through National Research Foundation of Korea funded by the Ministry of Education, Science and Technology. J.G. is a 'Ramón y Cajal' research fellow of the Spanish Ministry for Science and Innovation supported by (MICINN, Nr.CTQ2011-27317).*

## BIOGRAPHICAL INFORMATION

**Byeong-Kwan An** received his Ph.D. in Materials Science and Engineering with Prof. Soo Young Park from Seoul National University (2005). After a research associate position at the University of Oxford and the University of Queensland (Australia) with Paul Burn (2005−2010), he returned in 2010 to the Catholic University of Korea, where he is currently a faculty member in the Department of Chemistry. His current research focuses on conjugated semiconducting and organometallic materials for organic optoelectronics.

**Johannes Gierschner** received his Ph.D. in Physical Chemistry in Tübingen, Germany (2000). After a postdoctoral stay at the University of Mons (Belgium) and GeorgiaTech (United States), he joined IMDEA Nanoscience in 2008 as a senior researcher. Since 2009 he is a regular visiting researcher at SNU. His work integrates optical spectroscopy and computational chemistry to elucidate the structure−property relationships in conjugated organic materials.

**Soo Young Park** earned his Ph.D. (1988) in Fiber and Polymer Science and Engineering from Seoul National University. He was a senior researcher at the Korea Institute of Science and Technology (1985−1995). He joined Seoul National University as a faculty member in 1995 and was promoted and tenured as a full professor of Materials Science and Engineering in 2004. He was appointed as a fellow of the Korean Academy of Science and Technology in 2010. His research areas include the design and synthesis of molecular electronics/photonics materials.

## FOOTNOTES

*To whom correspondence should be addressed. E-mail: parksy@snu.ac.kr. Telephone: 82-2-880-8327. Fax: 82-2-886-8331.

## REFERENCES

1 Ajayaghosh, A.; Praveen, V. K. $\pi$-Organogels of Self-Assembled p-Phenylenevinylenes: Soft Materials with Distinct Size, Shape, and Functions. *Acc. Chem. Res.* **2007**, *40*, 644–656.

2 Cornil, J.; Beljonne, D.; Calbert, J.-P.; Brédas, J.-L. Interchain Interactions in Organic $\pi$-Conjugated Materials: Impact on Electronic Structure, Optical Response, and Charge Transport. *Adv. Mater.* **2001**, *13*, 1053–1067.

3 Gierschner, J.; Ehni, M; Egelhaaf, H.-J.; Milián Medina, B.; Beljonne, D.; Benmansour, H.; Bazan, G. C. Solid-State Optical Properties of Linear Polyconjugated Molecules: $\pi$-Stack Contra Herringbone. *J. Chem. Phys.* **2005**, *123*, 144914.

4 An, B.-K.; Kwon, S.-K.; Jung, S.-D.; Park, S. Y. Enhanced Emission and Its Switching in Fluorescent Organic Nanoparticles. *J. Am. Chem. Soc.* **2002**, *124*, 14410–14415.

5 Oelkrug, D.; Tompert, A.; Gierschner, J.; Egelhaaf, H.-J.; Hanack, M.; Hohloch, M.; Steinhuber., E. Tuning of Fluorescence in Films and Nanoparticles of Oligophenylenevinylenes. *J. Phys. Chem. B* **1998**, *102*, 1902–1907.

6 Karpfen, A.; Choi, C. H.; Kertesz, M. Single-Bond Torsional Potentials in Conjugated Systems: A Comparison of ab Initio and Density Functional Results. *J. Phys. Chem. A* **1997**, *101*, 7426–7433.

7 Lhost, O.; Brédas, J. L. Theoretical Study of Torsion Potentials in trans-Stilbene and Substituted trans-Stilbenes: Modeling Torsions in Poly(paraphenylene vinylene) and Derivatives. *J. Chem. Phys.* **1992**, *96*, 5279–5288.

8 Yoon, S.-J.; Chung, J. W.; Gierschner, J.; Kim, K. S.; Choi, M.-G.; Kim, D.; Park, S. Y. Multistimuli Two-Color Luminescence Switching via Different Slip-Stacking of Highly Fluorescent Molecular Sheets. *J. Am. Chem. Soc.* **2010**, *132*, 13675–13683.

9 Babu, S. S.; Kartha, K. K.; Ajayaghosh, A. Excited State Processes in Linear $\pi$-System-Based Organogels. *J. Phys. Chem. Lett.* **2010**, *1*, 3413–3424.

10 Liu, J.; Lam, J. W. Y.; Tang, B. Z. Aggregation-induced Emission of Silole Molecules and Polymers: Fundamental and Applications. *J. Inorg. Organomet. Polym. Mater.* **2009**, *19*, 249–285.

11 Babu, S. S.; Praveen, V. K.; Prasanthkumar, S.; Ajayaghosh, A. Self-Assembly of Oligo(para-phenylenevinylene)s through Arene-Perfluoroarene Interactions: $\pi$ Gels with Longitudinally Controlled Fiber Growth and Supramolecular Exciplex-Mediated Enhanced Emission. *Chem.—Eur. J.* **2008**, *14*, 9577–9584.

12 An, B.-K.; Kwon, S.-K.; Park, S. Y. Highly Sensitive Fluorescence Probes for Organic Vapors: On/off and Dual Color Fluorescence Switching. *Bull. Korean Chem. Soc.* **2005**, *26*, 1555–1559.

13 An, B.-K.; Lee, D.-S.; Lee, J.-S.; Park, Y.-S.; Song, H.-S.; Park, S. Y. Strongly Fluorescent Organogel System Comprising Fibrillar Self-assembly of Trifluoromethyl-Based Cyanostilbene Derivative. *J. Am. Chem. Soc.* **2004**, *126*, 10232–10233.

14 An, B.-K.; Gihm, S. H.; Chung, J. W.; Park, C. R.; Kwon, S.-K.; Park, S. Y. Color Tuned Highly Fluorescent Organic Nanowires/Nanofabrics: Easy Massive Fabrication and Molecular Structural Origin. *J. Am. Chem. Soc.* **2009**, *131*, 3950–3957.

15 Chung, J. W.; An, B.-K.; Kim, J. W.; Kim, J.-J.; Park, S. Y. Self-Assembled Perpendicular Growth of Organic Nanoneedles via Simple Vapor-Phase Deposition: One-Step Fabrication of a Superhydrophobic Surface. *Chem. Commun.* **2008**, 2998–3000.

16 Kim, J. H.; Watanabe, A.; Chung, J. W.; Jung, Y.; An, B.-K.; Tada, H.; Park, S. Y. All-Organic Coaxial Nanocables with Interfacial Charge-Transfer Layers: Electrical Conductivity and Light-Emitting-Transistor Behavior. *J. Mater. Chem.* **2010**, *20*, 1062–1064.

17 An, B.-K.; Kwon, S.-K.; Park, S. Y. Photopatterned Arrays of Fluorescent Organic Nanoparticles. *Angew. Chem., Int. Ed.* **2007**, *46*, 1978–1982.

18 Chung, J. W.; An, B.-K.; Hirato, F.; Kim, J. H.; Jinnai, H.; Park, S. Y. Selected-Area In Situ Generation of Highly Fluorescent Organic Nanowires Embedded in a Polymer Film: The Solvent-Vapor-Induced Self-Assembly Process. *J. Mater. Chem.* **2010**, *20*, 7715–7720.

19 Xie, W.; Li, Y.; Li, F.; Shen, F.; Ma, Y. Amplified Spontaneous Emission from Cyano Substituted Oligo(p-phenylene vinylene) Single Crystal with Very High Photoluminescent Efficiency. *Appl. Phys. Lett.* **2007**, *90*, 141110–1411103.

20 Kunzelman, J.; Kinami, M.; Crenshaw, B. R.; Protasiewicz, J. D.; Weder, C. Oligo (p-phenylene vinylene)s as A "New" Class of Piezochromic Fluorophores. *Adv. Mater.* **2008**, *20*, 119–122.

21 Tanaka, M.; Oki, Y.; Nagano, D.; An, B.-K.; Park, S. Y.; Maeda, M. Distributed feedback waveguide laser of organic nano-compound material. *Mol. Cryst. Liq. Cryst.* **2007**, *463*, 455–465.

22 Lim, S.-J.; An, B.-K.; Jung, S. D.; Chung, M.-A.; Park, S. Y. Photoswitchable Organic Nanoparticles and Polymer Film Employing Multifunctional Molecules with Enhanced Fluorescence Emission and Bistable Photochromism. *Angew. Chem., Int. Ed.* **2004**, *43*, 6346–6350.

23 Chung, J. W.; Yoon, S.-J.; Lim, S.-J.; An, B.-K.; Park, S. Y. Dual-Mode Switching in Highly Fluorescent Organogels: Binary Logic Gates with Optical/Thermal Inputs. *Angew. Chem., Int. Ed.* **2009**, *48*, 7030–7034.

24 Srinivasan, S.; Babu, P. A.; Mahesh, S.; Ajayaghosh, A. Reversible Self-Assembly of Entrapped Fluorescent Gelators in Polymerized Styrene Gel Matrix: Erasable Thermal Imaging via Recreation of Supramolecular Architectures. *J. Am. Chem. Soc.* **2009**, *131*, 15122–15123.

25 Kim, J. H.; Jung, Y.; Chung, J. W.; An, B.-K.; Park, S. Y. Fabrication of a Patterned Assembly of Semiconducting Organic Nanowires. *Small* **2009**, *5*, 804–807.

26 Bradley, D. D. C. Precursor-route Poly(p-phenylenevinylene): Polymer Characterisation and Control of Electronic Properties. *J. Phys. D: Appl. Phys.* **1987**, *20*, 1389–1410.

27 Chung, J. W.; Yang, H.; Singh, B.; Moon, H.; An, B.-K.; Lee, S. Y.; Park, S. Y. Single-Crystalline Organic Nanowires with Large Mobility and Strong Fluorescence Emission: A Conductive-AFM and Space-Charge-Limited-Current Study. *J. Mater. Chem.* **2009**, *19*, 5920–5925.

28 Kim, J. H.; Chung, J. W.; Jung, Y.; Yoon, S.-J.; An, B.-K.; Huh, H. S.; Lee, O. W.; Park, S. Y. High Performance n-Type Organic Transistors Based on Distyrylthiophene Derivative. *J. Mater. Chem.* **2010**, *20*, 10103–10106.